

Multinuclear Cu(II) Schiff Base Complex as Efficient Catalyst for the Chemical Coupling of CO₂ and Epoxides: Synthesis, X-ray Structural Characterization and Catalytic Activity

Mahmut Ulusoy · Onur Şahin · Ahmet Kılıc ·
Orhan Büyükgüngör

Received: 25 August 2010 / Accepted: 24 November 2010 / Published online: 14 December 2010
© Springer Science+Business Media, LLC 2010

Abstract The synthesis, X-ray structure, spectroscopic and catalytic properties of sterically hindered Schiff-base ligands ($L_1H = N$ -[allylamine]-3,5-di-*tert*-butyl salicylaldimine, $L_2H=N$ -[2-amino-5-methyl pyridine]-3,5-di-*tert*-butyl salicylaldimine and $L_3H=N$ -[2-amino-6-methyl pyridine]-3,5-di-*tert*-butyl salicylaldimine), and their mononuclear Cu(II) complex for L_1H with multinuclear Cu(II) complexes for L_2H and L_3H , were described. The copper(II) complexes of these ligands were synthesized by treating an methanolic solution of the appropriate ligand with an appropriate amount of $CuCl_2 \cdot 2H_2O$. The ligands and their copper(II) complexes were characterized by FT-IR, UV–Vis, ¹H-NMR, elemental analysis, measurement of room temperature magnetic moment, and X-ray structural determination. The reaction of the L_2H and L_3H ligands in a 1:1 mol ratio with $CuCl_2 \cdot 2H_2O$ afforded ionic copper metal(II) complexes in the presence of NEt₃. The Cu(II) metal complexes tested as catalysts for the formation of cyclic organic carbonates from carbon dioxide and liquid epoxides which served as both reactant and solvent. $[Cu_3(L_2)_4]Cl_2 \cdot CuCl_2$ complex which has 5-methyl substituent on the pyridine ring showed high catalytic activity for chemical coupling carbon dioxide with epoxides (propylene oxide (PO), epichlorohydrine (EC) and 1,2-epoxy butane (EB)) selectively.

Keywords Schiff base · Cu(II) complexes · X-ray structure · CO₂ · Cyclic carbonate

1 Introduction

In the current global climate, with high oil prices and increasing concern over global warming, and consumption petroleum resources, the development of renewable carbon sources is of the utmost importance. CO₂ is a particularly attractive alternative feedstock as it is inexpensive, highly naturally abundant, and the byproduct of many industrial processes, including combustion [1]. The reactions of CO₂ with metal complexes has been extensively studied, revealing potential pathways for catalytic reactions [2–5]. However the thermodynamic stability of CO₂ has hampered its utility as a reagent for chemical synthesis; in fact its high stability makes it an ideal medium for many chemical processes [2, 6]. In particular, the catalytic coupling of CO₂ with heterocycles has received considerable attention over the past 35 years [1, 7–10]. A majority of these publications involve the reaction of CO₂ with epoxides to generate polycarbonates and/or cyclic carbonates. Cyclic carbonates are used excellent aprotic polar solvents, electrolytes in secondary batteries, precursors for polycarbonates and biomedical applications [11–14]. These products have a high boiling point and have therefore found many applications as solvents. However, the carbamates can be obtained via synthesis of ammonia or amines. The carbamates can then be converted into polyurethane, a versatile material with a high commercial value [15–18].

There is a continuing interest in copper metal complexes of Schiff bases because of the presence of both nitrogen and oxygen donor atoms in the backbones of these ligands [19]. Lots of studies about metal based complexes as the

M. Ulusoy (✉) · A. Kılıc
Department of Chemistry, University of Harran, 63190
Sanliurfa, Turkey
e-mail: ulusoymahmut@harran.edu.tr

O. Şahin · O. Büyükgüngör
Department of Physics, Ondokuz Mayıs University, 55139
Kurupelit, Samsun, Turkey

catalysts for the catalytic conversion of CO₂ into valuable organic products were published in recent years [20–22].

This study aims at obtaining new coordinative compounds with similar properties. Therefore, the present manuscript describes the synthesis, structural characterization and the catalytic activity of three new steric hindered Schiff base ligands ($L_1H=N$ -[allylamine]-3,5-di-*t*-butyl salicylaldimine, $L_2H=N$ -[2-amino-5-methyl pyridine]-3,5-di-*t*-butyl salicylaldimine and $L_3H=N$ -[2-amino-6-methyl pyridine]-3,5-di-*t*-butyl salicylaldimine) involving nitrogen and oxygen donor sites and their Cu(II) metal complexes derivatives with general formula presented Scheme 2.

2 Experimental

2.1 Materials and Measurements

All reagents and solvents were of reagent-grade quality and obtained from commercial suppliers (Aldrich or Merck). The elemental analyses were carried out in the Laboratory of the Scientific and Technical Research Council of Turkey (TUBITAK). IR spectra were recorded on a Perkin Elmer Spectrum 100 FT-IR Spectrometer as KBr pellets. ¹H-NMR spectra were recorded on a Varian AS-400 MHz instrument CDCl₃ at room temperature. Chemical shifts were given in parts per million from tetramethylsilane. Magnetic Susceptibilities were determined on a Sherwood Scientific Magnetic Susceptibility Balance (Model MK1) at room temperature (20 °C) using Hg[Co(SCN)₄] as a calibrant; diamagnetic corrections were calculated from Pascal's constants [23]. Electronic spectral studies were conducted on a Varian Carry 100 model UV-visible spectrophotometer at the wavelength range of 200–1100 nm. Melting points were measured in open capillary tubes with an Electrothermal 9100 melting point apparatus and uncorrected. Catalytic tests were performed in a PARR 4843 50 mL stainless pressure reactor.

2.2 Synthesis of Ligands (L_1H , L_2H and L_3H):

N-[allylamine]-3,5-di-*t*-butyl salicylaldimine (L_1H), *N*-[2-amino-5-methyl pyridine]-3,5-di-*tert*-butyl salicylaldimine (L_2H) and *N*-[2-amino-6-methyl pyridine]-3,5-di-*tert*-butyl salicylaldimine (L_3H) ligands were synthesized by the reaction of 4.3 mmol (1.0 g) 3,5-di-*tert*-butyl-2-hydroxybenzaldehyde in 30 mL absolute methanol with 4.3 mmol (0.25 g) allylamine for L_1H , 4.3 mmol (0.46 g) 2-amino-5-methyl-pyridine for L_2H and 4.3 mmol (0.46 g) 2-amino-6-methyl-pyridine for L_3H in 15 mL absolute methanol. Also, 3–4 drops of formic acid were added as catalyst. The mixtures were refluxed for 3 h. During this

time a yellow solid precipitated from solution which was isolated by filtration, washed with cold methanol and dried vacuum. Then, the products were recrystallized from ethanol. The products are soluble in common solvents such as CHCl₃, CH₃CH₂OH, DMF and DMSO.

For (L_1H) ligand: Color: Yellow; m.p: 102 °C; Yield (%): 88; Anal. Calc. for C₁₈H₂₇NO (F.W: 273.4 g/mol): C, 79.07; H, 9.95; N, 5.12. Found: C, 79.12; H, 9.89; N, 5.15%. ¹H NMR (400 MHz, CDCl₃, Me₄Si, ppm): δ = 13.62 (s, 1H, –OH, D-exchangeable), δ = 8.21 (s, 1H, HC=N), δ = 7.41 (s, 1H, Ar–CH), δ = 7.19 (s, 1H, Ar–CH), δ = 6.04–5.98 (m, 1H, C=CH), δ = 5.28–5.17 (m, 2H, C=CH₂), δ = 4.22 (s, 2H, N–CH₂), δ = 1.43 (s, 9H, C–CH₃) and δ = 1.26 (s, 9H, C–CH₃). IR (KBr pellets, $\nu_{\text{max}}/\text{cm}^{-1}$): 3520–2480 $\nu(\text{OH}\cdots\text{N})$, 3044 $\nu(\text{Ar–CH})$, 2955–2785 $\nu(\text{Alip–CH})$, 1630 $\nu(\text{C=N})$, 1458–1432 $\nu(\text{C=C})$, 1174 $\nu(\text{C–O})$. UV–Vis (λ_{max} , nm, * = shoulder peak): 240, 264, 331 and 417* (in CHCl₃).

For (L_2H) ligand: Color: Yellow; m.p: 144 °C; Yield (%): 91; Anal. Calc. for C₂₁H₂₈N₂O (F.W: 324.5 g/mol): C, 77.74; H, 8.70; N, 8.63. Found: C, 77.72; H, 8.64; N, 8.57%. ¹H NMR (400 MHz, CDCl₃, Me₄Si, ppm): δ = 13.94 (s, 1H, –OH, D-exchangeable), δ = 9.48 (s, 1H, HC=N), δ = 8.32 (s, 1H, Ar–CH), δ = 7.59–7.56 (d, 1H, J=12, Ar–CH), δ = 7.47 (s, 1H, Ar–CH), δ = 7.34 (s, 1H, Ar–CH), δ = 7.21 (s, 1H, Ar–CH), δ = 2.41 (s, 3H, Ar–CH₃), δ = 1.46 (s, 9H, C–CH₃) and δ = 1.28 (s, 9H, C–CH₃). IR (KBr pellets, $\nu_{\text{max}}/\text{cm}^{-1}$): 3629 $\nu(\text{OH})$, 3052 $\nu(\text{Ar–CH})$, 2958–2742 $\nu(\text{Alip–CH})$, 1613 $\nu(\text{C=N})$, 1471–1458 $\nu(\text{C=C})$, 1170 $\nu(\text{C–O})$. UV–Vis (λ_{max} , nm, * = shoulder peak): 241, 281, 317, 368, 484* (in CHCl₃).

For (L_3H) ligand: Color: Yellow; m.p: 106 °C; Yield (%): 93; Anal. Calc. for C₂₁H₂₈N₂O (F.W: 324.5 g/mol): C, 77.74; H, 8.70; N, 8.63. Found: C, 77.68; H, 8.67; N, 8.66%. ¹H NMR (400 MHz, CDCl₃, Me₄Si, ppm): δ = 13.96 (s, 1H, –OH, D-exchangeable), δ = 9.81 (s, 1H, HC=N), δ = 7.81–7.79 (d, 1H, J = 12, Ar–CH), δ = 7.60 (s, 1H, Ar–CH), δ = 7.47 (s, 1H, Ar–CH), δ = 7.35 (s, 1H, Ar–CH), δ = 7.22 (s, 1H, Ar–CH), δ = 2.38 (s, 3H, Ar–CH₃), δ = 1.47 (s, 9H, C–CH₃) and δ = 1.29 (s, 9H, C–CH₃). IR (KBr pellets, $\nu_{\text{max}}/\text{cm}^{-1}$): 3580–2528 $\nu(\text{OH}\cdots\text{N})$, 3048 $\nu(\text{Ar–CH})$, 2954–2749 $\nu(\text{Alip–CH})$, 1612 $\nu(\text{C=N})$, 1550–1457 $\nu(\text{C=C})$, 1171 $\nu(\text{C–O})$. UV–Vis (λ_{max} , nm, * = shoulder peak): 241, 279, 317, 368, 480* (in CHCl₃).

2.3 Synthesis of the Cu(II) Metal Complexes

0.50 g, 1.84 mmol ligand (L_1H), 0.50 g, 1.54 mmol ligand (L_2H) or 0.50 g, 1.54 mmol ligand (L_3H) was dissolved in methanol (30 cm³). A solution of 0.16 g, 0.92 mmol of the metal salt [CuCl₂·2H₂O] for mononuclear [Cu(L_1)₂] complex and 0.26 g, 1.54 mmol of the metal salt [CuCl₂·2H₂O] for multinuclear [Cu₃($L_{2,3}$)₄]Cl₂·CuCl₂ complexes in

methanol (20 cm^3), was added dropwise under a N_2 atmosphere with continuous stirring. A few drops of NEt_3 was added while stirring. The stirred mixtures were then heated to the reflux temperature for 3 h and were maintained at this temperature. Then, the mixture was evaporated to a volume of 5 mL in vacuum and left to cool to room temperature. The precipitated products were filtered in vacuum and washed with a small amount of ethanol and water. The products were recrystallized from CH_2Cl_2 -hexane. The resulting green solutions were cooled to room temperature and allowed to stand for two week during which green crystals formed. The crystals were filtered off, washed with cold methanol and dried in air.

For $[\text{Cu}(\text{L}_1)_2]$: Color: Green; m.p: $225\text{ }^\circ\text{C}$; Yield (%): 75; Anal. Calc. for $[\text{C}_{42}\text{H}_{54}\text{N}_4\text{O}_2\text{Cu}]$ (F.W: 608.4 g/mol): C, 71.07; H, 8.62; N, 4.60. Found: C, 70.94; H, 8.71; N, 4.48%. IR (KBr pellets, $\nu_{\text{max}}/\text{cm}^{-1}$): 3042 $\nu(\text{Ar}-\text{CH})$, 2955–2833 $\nu(\text{Alif}-\text{CH})$, 1609 $\nu(\text{C}=\text{N})$, 1481–1422 $\nu(\text{C}=\text{C})$, 1168 $\nu(\text{C}-\text{O})$, 519 $\nu(\text{Cu}-\text{N})$ and 486 $\nu(\text{Cu}-\text{O})$. $\mu_{\text{eff}} = 1.73$ [B.M]. UV-Vis (λ_{max} , nm, * = shoulder peak): 242, 269, 389, 485*, 704* (in CHCl_3).

For $[\text{Cu}_3(\text{L}_2)_4]\text{Cl}_2 \cdot \text{CuCl}_2$: Color: Dark Green; m.p: $> 300\text{ }^\circ\text{C}$; Yield (%): 72; Anal. Calc. for $[\text{C}_{84}\text{H}_{110}\text{N}_8\text{O}_4\text{Cl}_4\text{Cu}_3]$ (F.W: 1628.3 g/mol): C, 61.96; H, 6.81; N, 6.88. Found: C, 61.83; H, 6.72; N, 6.72%. IR (KBr pellets, $\nu_{\text{max}}/\text{cm}^{-1}$): 3048 $\nu(\text{Ar}-\text{CH})$, 2954–2826 $\nu(\text{Alif}-\text{CH})$, 1605 $\nu(\text{C}=\text{N})$, 1460–1435 $\nu(\text{C}=\text{C})$, 1165 $\nu(\text{C}-\text{O})$, 537 $\nu(\text{Cu}-\text{N})$ and 490 $\nu(\text{Cu}-\text{O})$. $\mu_{\text{eff}} = 1.78$ [B.M]. UV-Vis (λ_{max} , nm, * = shoulder peak): 241, 306, 355, 463, 511*, 734* (in CHCl_3).

For $[\text{Cu}_3(\text{L}_3)_4]\text{Cl}_2 \cdot \text{CuCl}_2$: Color: Dark green; m.p: $264\text{ }^\circ\text{C}$; Yield (%): 70; Anal. Calc. for $[\text{C}_{84}\text{H}_{110}\text{N}_8\text{O}_4\text{Cl}_4\text{Cu}_3]$ (F.W: 1628.3 g/mol): C, 61.96; H, 6.81; N, 6.88. Found: C, 61.88; H, 6.79; N, 6.74%. IR (KBr pellets, $\nu_{\text{max}}/\text{cm}^{-1}$): 3046 $\nu(\text{Ar}-\text{CH})$, 2955–2868 $\nu(\text{Alif}-\text{CH})$, 1603 $\nu(\text{C}=\text{N})$, 1461–1423 $\nu(\text{C}=\text{C})$, 1166 $\nu(\text{C}-\text{O})$, 529 $\nu(\text{Cu}-\text{N})$ and 472 $\nu(\text{Cu}-\text{O})$. $\mu_{\text{eff}} = 1.78$ [B.M]. UV-Vis (λ_{max} , nm, * = shoulder peak): 215, 241, 269, 368, 415, 518*, 728* (in CHCl_3).

2.4 General Procedure for the Cycloaddition of Epoxides to CO_2

A 50 mL stainless pressure reactor was charged with Cu(II) complexes (1.125×10^{-5} mol), epoxide (4.5×10^{-2} mol), 4-dimethylamino-pyridine (DMAP) (11 mg, 9.0×10^{-5} mol) or NEt_3 (0.013 mL, 9.0×10^{-5} mol), if used CH_2Cl_2 (5.0 mL). The reaction vessel was placed under a constant pressure of carbon dioxide for 2 min to allow the system to equilibrate (except propylene oxide (PO) as the epoxide) and CO_2 was charged into the autoclave with desired pressure, then heated to the desired temperature. The pressure was kept constant during the

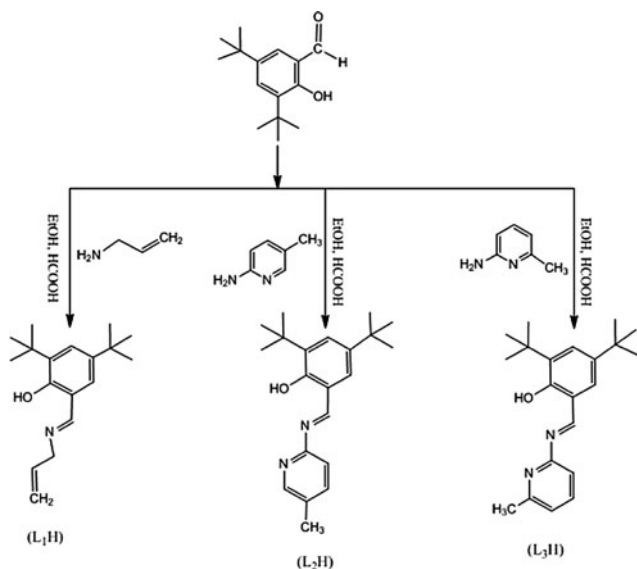
reaction. The vessel was then cooled to 5–10 °C in ice bath after the expiration of the desired time of reaction. The pressure was released, then, the excess gases were vented. The yields of epoxides to corresponding cyclic carbonates were determined by comparing the ratio of product to substrate in the ^1H NMR spectrum of an aliquot of the reaction mixture.

2.5 Crystallography

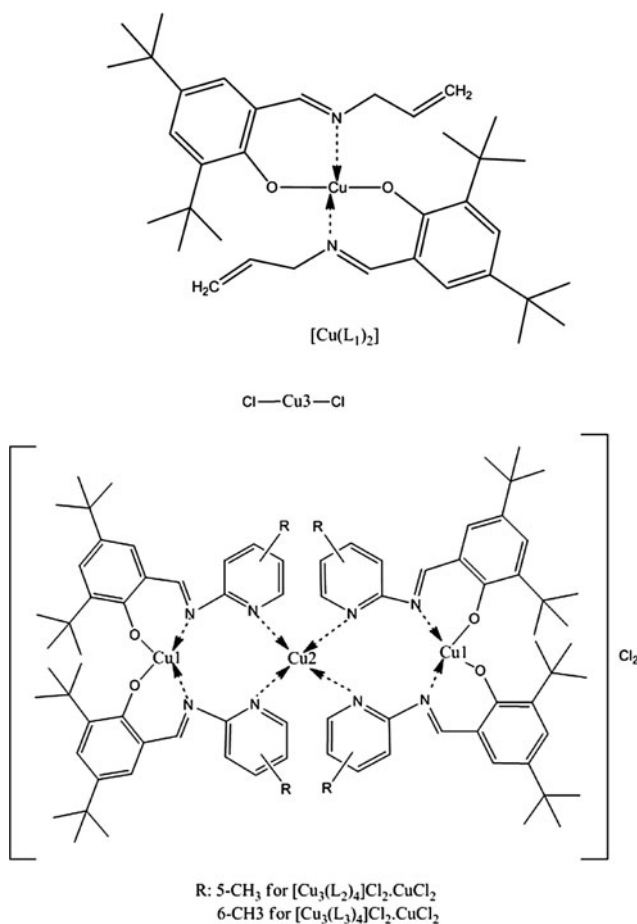
A dark-green colour crystal of the copper complex, suitable for data collection was mounted on a glass fiber and data collection was performed on a STOE IPDS II diffractometer with graphite monochromated Mo K_α radiation at 296 K. Details of crystal data, data collection and refinement were given in Table 2. The structure was solved by direct-methods using SHELXS-97 [24] and refined by full-matrix least-squares methods on F^2 using SHELXL-97 from within the WINGX [25] suite of software. All non-hydrogen atoms were refined with anisotropic parameters. Hydrogen atoms bonded to carbon were placed in calculated positions ($\text{C}-\text{H} = 0.93\text{--}0.96\text{ \AA}$) and treated using a riding model with $U = 1.2$ times the U value of the parent atom for CH and CH_3 . The molecular drawing was obtained using ORTEP-III [26]. Geometric calculations were performed on PLATON [27].

3 Results and Discussion

The ligands (L_1H , L_2H and L_3H) were prepared in moderate yields by refluxing the 3,5-di-*tert*-butyl-2-hydroxybenzaldehyde with allylamine, 2-amino-5-methylpyridine or 2-amino-6-methyl-pyridine (one equivalent



Scheme 1 Synthetic route for preparation of proposed ligands (L_nH)



Scheme 2 The structure of the proposed Cu(II) metal complexes

ratio) in absolute methanol (Scheme 1). The isolated ligands were characterized by their elemental analysis, melting point, FT-IR, UV-Vis and ¹H-NMR spectroscopy. The copper metal complexes (Scheme 2) were synthesized by treating $\text{CuCl}_2\cdot 2\text{H}_2\text{O}$ with one or two equivalents of the corresponding ligand in methanol at reflux temperature. The Cu(II) metal complexes are single crystalline or powder-like and they are stable at atmospheric conditions. To confirm the identity of the pre-catalysts prepared in the present work, a variety of techniques including elemental analysis, infrared spectroscopy, UV-Vis spectroscopy, X-ray structural determination for $[\text{Cu}_3(\text{L}_3)_4]\text{Cl}_2\cdot\text{CuCl}_2$ complex and magnetic susceptibility (μ_{eff} , BM) have been utilized. The metal to ligand ratios in the mono and multinuclear Cu(II) metal complexes were found to be 1:2 or 4:4 (Scheme 2). Results are presented in the experimental section.

3.1 NMR Spectra

The ¹H-NMR spectral data of the salen ligands were recorded in CHCl_3 solution using tetramethylsilane (TMS) as internal standard. The ¹H NMR spectra of the ligands and the

chemical shifts of the different types of protons were listed in experimental section. The proton NMR spectra of the free ligands show a peak as singlet at 13.62 ppm for L_1H , at 13.94 ppm for L_2H and at 13.96 ppm for L_3H , respectively. The peak corresponding to this proton disappears while addition a few drops of D_2O . The chemical shifts observed at $\delta = 8.21$ ppm for L_1H , at $\delta = 9.48$ ppm for L_2H and at $\delta = 9.81$ ppm for (L_3H) is assigned to the proton of azomethine ($\text{CH}=\text{N}$) as singlet [28, 29]. It is remarkable to see that the downfield chemical shift ($\delta = 9.48$ or 9.81 ppm) corresponds to the azomethine proton of the pyridine CH_3 group, which has the high electron donating power, while the upperfield value ($\delta = 8.21$ ppm) is of the allyl group with the high electron withdrawing power. Thus, it can be concluded that the position of the azomethine proton is strongly affected by the electron withdrawing/donating character of the groups on the aryl ring and double bound. Also, the protons of the *tert*-butyl groups of ligands exhibit singlet peak at $\delta = 1.43$ and 1.26 ppm for L_1H , $\delta = 1.46$ and 1.28 ppm for L_2H , and $\delta = 1.47$ and 1.29 ppm for L_3H , indicating that the *tert*-butyl protons of these compounds are magnetically nonequivalent [30].

3.2 IR Spectra

The IR spectra of the Cu(II) complexes are compared with those of the free ligand in order to determine the coordination sites that may be involved in chelation. There are some guide peaks in the spectra of the ligands, which are of good help for achieving this goal. The position and/or the intensities of these peaks are expected to be changed upon chelation. Coordination of the steric hindered ligands to the metal through the nitrogen atom is expected to reduce the electron density in the azomethine link and lower the $\nu(\text{C}=\text{N})$ absorption frequency. The very strong and sharp bands located at 1630–1612 cm^{-1} are assigned to the $\nu(\text{C}=\text{N})$ stretching vibrations of the azomethine of the ligands. These bands are shifted 21–8 cm^{-1} to a lower wavenumber which supports the participation of the azomethine group of these ligands in binding to the copper ion [31–33]. A strong peak observed at range 1174–1170 cm^{-1} in the free ligands has been assigned to phenolic C–O stretching. On the complexation this band is shifted to a lower frequency range 1168–1165 cm^{-1} , indicating coordination through the phenolic oxygen. The coordination of the azomethine nitrogen, phenolic oxygen for $[\text{Cu}(\text{L}_1)_2]$ complex and azomethine nitrogen, phenolic oxygen and pyridine nitrogen for $[\text{Cu}_3(\text{L}_2)_4]\text{Cl}_2\cdot\text{CuCl}_2$ and $[\text{Cu}_3(\text{L}_3)_4]\text{Cl}_2\cdot\text{CuCl}_2$ complexes are further supported by the appearance of peaks at range 537–519 cm^{-1} and at range 490–472 cm^{-1} due to $\nu(\text{Cu} \leftarrow \text{O})$ and $\nu(\text{Cu} \leftarrow \text{N})$ stretching vibrations that are not observed in the infrared spectra of the ligands [34]. Thus, it is clear that the ligands

L_1H , L_2H and L_3H are bonded to the per copper metal ion in a N_2O_2 (for L_1H) or N_2O_2 with N_4 fashion (for L_2H and L_3H) through the deprotonated phenolate oxygen, pyridine nitrogen and salicylaldimine nitrogen.

3.3 UV–Vis Spectra

Electronic spectra of ligands (L_nH) and their mono- or multinuclear Cu(II) metal complexes have been recorded in the 200–1100 nm range in $CHCl_3$ solution and their corresponding data are given in experimental part. In the electronic spectra of the ligands and their Cu(II) complexes, the wide range bands seem to be due to both the $\pi \rightarrow \pi^*$ and $n \rightarrow \pi^*$ of $C=N$ chromophore or charge-transfer transition arising from π electron interactions between the metal and ligand which involves either a metal-to-ligand or ligand-to-metal electron transfer and $d-d$ transitions [35–37]. The electronic spectra of the free ligands in $CHCl_3$ showed strong absorption bands in the ultraviolet region (264–368 nm) that could be attributed respectively to the $\pi \rightarrow \pi^*$ and $n \rightarrow \pi^*$ transitions in the benzene ring or azomethine ($-C=N$) groups. The free ligands also exhibited different absorption bands between 240–241 nm and 417–484 nm that attributed to the $n \rightarrow \pi^*$ and $n \rightarrow \sigma^*$ transitions [38]. In the spectra of the mono- and multinuclear Cu(II) complexes, the position and intensity of the absorption band characteristic of the ligand appeared to be modified with respect to those of the free ligand. Also, these spectra presented new bands between 518–511 and 734–704 nm that were characteristic of formed Cu(II) complexes. The absorption bands located in the 485–415 nm region were attributed to the $d \rightarrow \pi^*$ charge-transfer transitions, which overlap with the $\pi \rightarrow \pi^*$ and $n \rightarrow \pi^*$ transitions of the ligands [38]. The new absorption bands observed at lower energy and in lower intensities between 518–511 and 734–704 nm may be attributed to the $d-d$ transitions ($d_{xy} \rightarrow d_{x^2-y^2}$ and $d_{z^2} \rightarrow d_{x^2-y^2}$). These modifications in shifts and intensity for the absorption bands supported the coordination of the ligand to the central Cu(II) ion [38].

Table 2 Crystal data and structure refinement parameters for $[Cu_3(L_2)_4]Cl_2 \cdot CuCl_2$

Empirical formula	$C_{84}H_{108}Cu_4N_8O_4Cl_4$
Formula weight	1689.74
Temperature (K)	296
Wavelength (Å)	0.71073
Crystal system	Monoclinic
Space group	$C\ 2/c$
Unit cell dimensions	
a (Å)	12.9385(5)
b (Å)	24.6741(7)
c (Å)	28.7391(11)
α (°)	90
β (°)	93.834(3)
γ (°)	90
Volume (Å 3)	9154.3(6)
Z	4
D_{calc} (Mg/m $^{-3}$)	1.226
Absorption coefficient (mm $^{-1}$)	1.08
F(000)	3536
Crystal size (mm)	0.41 × 0.31 × 0.21
θ range for data collection (°)	1.4–26.1
Independent reflection	9005
Collected reflection	63,499
Absorption correction	Integration
T_{\min}	0.660
T_{\max}	0.841
R_{int}	0.097
h	–15 → 15
k	–30 → 30
l	–35 → 35
Refinement method	Full-matrix least-squares on F^2
wR(F^2)	0.118
Goodness-of-fit on F^2	0.92
Final R indices [$I > 2\sigma(I)$]	0.045
R indices (all data)	0.084
(Δ/σ) _{max}	0.003
$\Delta\rho_{\max}$ (e Å $^{-3}$)	0.45
$\Delta\rho_{\min}$ (e Å $^{-3}$)	–0.62

Table 1 Selected bond lengths (Å) and angles (°) for the copper complex with e.s.d.s. in parameters

O1–Cu1	1.899 (2)	N3–Cu2	2.148 (2)	C16–N1	1.411 (4)
O2–Cu1	1.911 (2)	N4–Cu2	2.131 (2)	C28–N2	1.297 (4)
N1–Cu1	1.936 (2)	C7–N1	1.304 (4)	C37–N2	1.411 (4)
N2–Cu1	1.936 (2)	O2–Cu1–N2	91.45 (9)	Cu1 ⁱ –Cu2–Cu1	175.94 (3)
O1–Cu1–O2	153.03 (10)	N1–Cu1–N2	157.94 (11)	C11–Cu3–C11 ⁱ	178.83 (8)
O1–Cu1–N1	92.30 (9)	N4–Cu2–N3	97.28 (9)	N4–Cu2–N3 ⁱ	144.55 (10)
O2–Cu1–N1	94.50 (10)	N4–Cu2–N4 ⁱ	94.60 (13)	O1–Cu1–N2	91.96 (9)

Symmetry code: ⁱ 1– x , y , 1/2– z

Table 3 Hydrogen bonds and $\pi\cdots\pi$ interactions for $[\text{Cu}_3(\text{L}_2)_4]\text{Cl}_2\cdot\text{CuCl}_2$

D-H…A	D-H (Å)	H…A (Å)	D…A (Å)	D-H…A (°)
C9–H9B…O1	0.96	2.38	3.010(4)	123
C10–H10A…O1	0.96	2.34	2.977(5)	123
C30–H30A…O2	0.96	2.32	2.966(5)	124
C31–H31B…O2	0.96	2.41	3.039(5)	122
C7–H7…Cl1	0.93	2.88	3.748(3)	156
C38–H38…Cl1 ⁱⁱ	0.93	2.90	3.791(4)	160
X…H(<i>I</i>)	Cg(<i>J</i>)	H…Cg (Å)	X–H…Cg (°)	
C(9)–H(9B)	Cg(4)	2.7986	142.68	
C(21)–H(21A)	Cg(5) ⁱ	2.7876	134.75	
C(31)–H(31B)	Cg(3)	2.9119	143.26	
C(42)–H(42A)	Cg(6) ⁱ	2.9068	164.79	

Cg(3): N3–C16–C17–C18–C19–C20, Cg(4): N4–C37–C38–C39–C40–C41, Cg(5): C1–C2–C3–C4–C5–C6, Cg(6): C22–C23–C24–C25–C26–C27

Symmetry code: ⁱ $-x, y, 1/2-z$; ⁱⁱ $1/2-x, y-1/2, 1/2-z$

3.4 Magnetic Moments

Magnetic susceptibility measurements provide sufficient data to characterize the structure of the metal complexes. Magnetic moments measurements of compounds were carried out at 25 °C. The room temperature effective magnetic moments (μ_{eff}) of all the complexes were measured on polycrystalline samples after necessary diamagnetic corrections using Pascal's table. The room temperature

magnetic moment of all the Cu(II) complexes showed a normal magnetic moment (in experimental part). The magnetic moment data of the Cu(II) complexes range 1.78–1.73 B.M. for per Cu(II) molecule, corresponding to one unpaired electron [39]. It is obvious that the Cu(II) complexes do not possess antiferromagnetic properties at room temperature. So, the Cu(II) complexes may be considered to have tetragonal geometry.

3.5 X-ray Structural Determination

The compound of $[\text{Cu}_3(\text{L}_2)_4]\text{Cl}_2\cdot\text{CuCl}_2$ (Fig. 2) crystallizes with $Z'=1/2$ in the space group C2/c, and important interatomic data are listed in Table 1. The crystallographic data are summarized in Table 2. Details of hydrogen-bonds and C–H…π interactions are given in Table 3. Compound $[\text{Cu}_3(\text{L}_2)_4]\text{Cl}_2\cdot\text{CuCl}_2$, has got three Cu(II) ions. Firstly, the Cu2 atom is located on a symmetry center and is coordinated by four N atoms (N3, N4, N3ⁱ, N4ⁱ) [Symmetry code: $i = -x, y, 1/2-z$] from pyridine groups of two L₂H ligand. Secondly, Cu1 atom has got four coordination number with two phenolate O atom (O1 and O2) and two azomethine-N atoms (N1 and N2) from two L₂H ligands. Finally, the Cu3 atom is located on a symmetry center and is coordinated by two Cl atoms (Cl1 and Cl1ⁱ) [Symmetry code: $i = -x, y, 1/2-z$]. Furthermore, there are two Cl atoms (Cl2 and Cl3) which are not coordinated (Fig. 1). Molecules of (I) are linked into sheets by a combination of C–H…Cl hydrogen bonds (Table 3). Atom C7 in the

Fig. 1 Molecular structure of $[\text{Cu}_3(\text{L}_2)_4]\text{Cl}_2\cdot\text{CuCl}_2$, asymmetric unit. [Symmetry code: $i = -x, y, 1/2-z$]

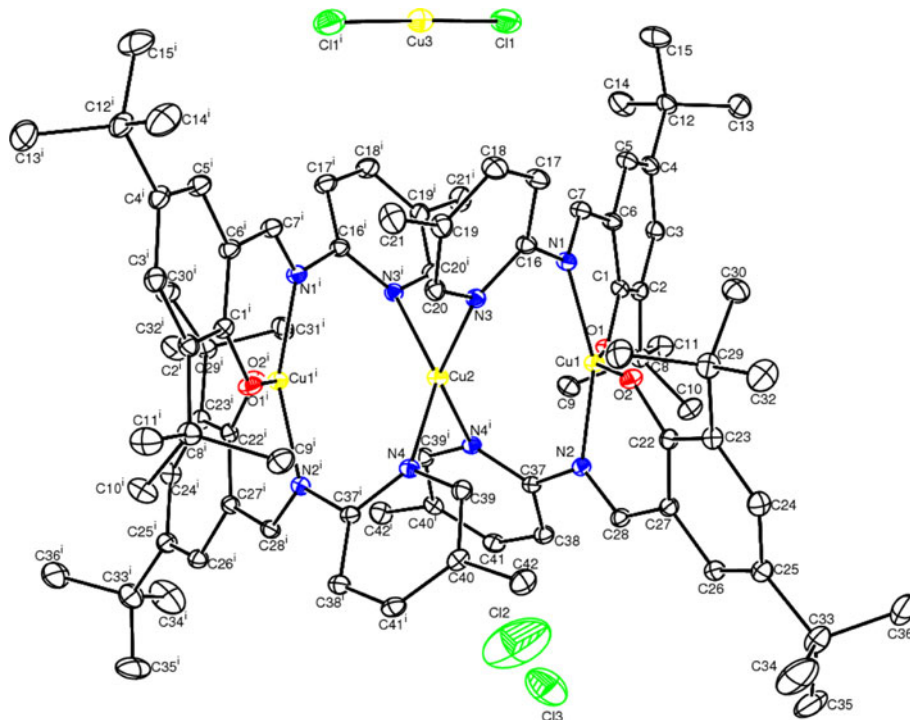


Fig. 2 Part of the crystal structure of $[\text{Cu}_3(\text{L}_2)_4\text{Cl}_2 \cdot \text{CuCl}_2$, showing the formation of $\text{R}_2^2(12)$ and $\text{R}_6^4(30)$ rings. H atoms not involved in these interactions have been omitted for clarity

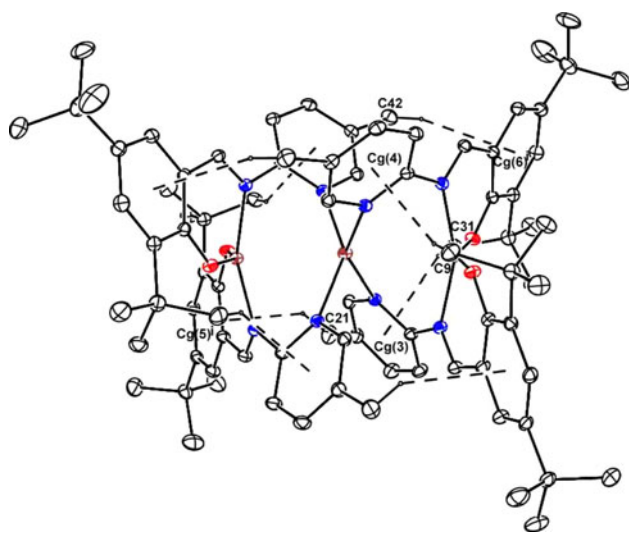
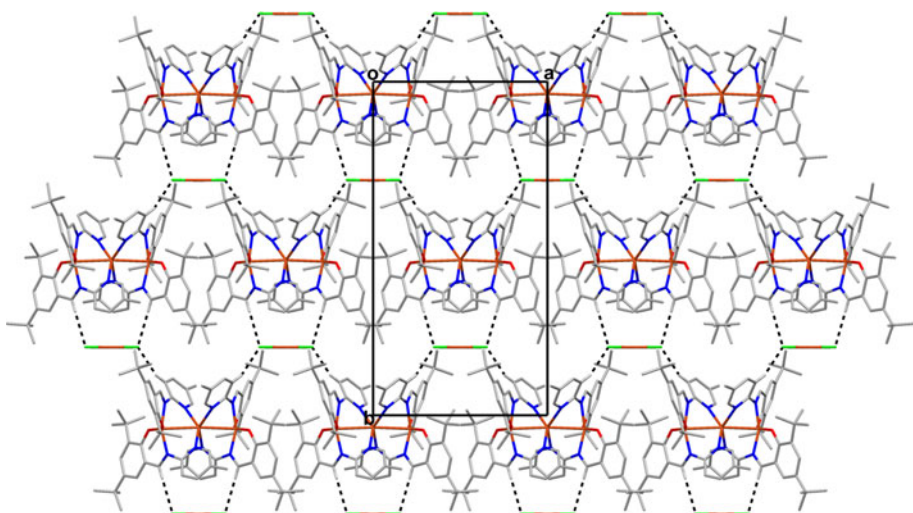


Fig. 3 Part of the crystal structure of $[\text{Cu}_3(\text{L}_2)_4\text{Cl}_2 \cdot \text{CuCl}_2$, showing the $\text{C}-\text{H}\cdots\pi$ interactions. [Symmetry code: $i = 1-x, y, 1/2-z$]

reference molecule at (x, y, z) acts as hydrogen-bond donor, to atom Cl1 in the molecule at (x, y, z) , so forming a centrosymmetric $\text{R}_2^2(12)$ ring [40]. Similarly, atom C38 in the reference molecule at (x, y, z) acts as hydrogen-bond donor, to atom Cl1 in the molecule at $(1/2-x, y-1/2, 1/2-z)$, so forming a $\text{C}_2^2(9)$ chain running parallel to the $[0-10]$ direction. The combination of $\text{C}-\text{H}\cdots\text{Cl}$ hydrogen bonds generates $\text{R}_6^4(30)$ rings parallel to the ab plane (Fig. 2). Compound (I) also contains two intramolecular $\text{C}-\text{H}\cdots\pi$ interactions and two intermolecular $\text{C}-\text{H}\cdots\pi$ interactions (Table 3). The intramolecular $\text{C}-\text{H}\cdots\pi$ interactions produce S(10) rings. The first is the intermolecular $\text{C}-\text{H}\cdots\pi$ interaction, C21 atom in the molecule at (x, y, z) acts as a hydrogen-bond donor to the benzene ring C1-C6 in the molecule at $(1-x, y, 1/2-z)$, so forming a $\text{R}_1^1(12)$ ring. The second is the C42 atom in the molecule at (x, y, z) acts as a

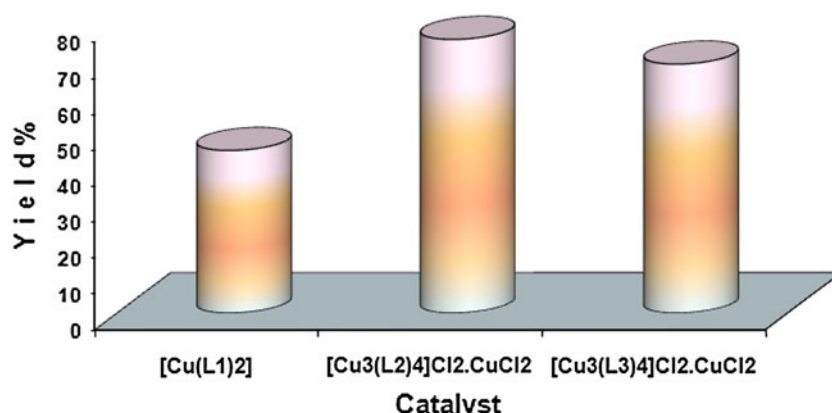
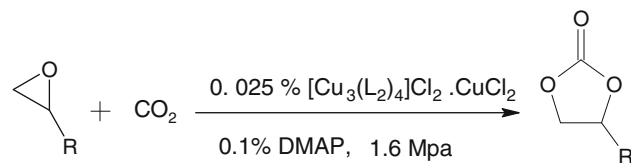
hydrogen-bond donor to the benzene ring C22-C27 in the molecule at $(1-x, y, 1/2-z)$, so forming a $\text{R}_1^1(12)$ ring (Fig. 3).

3.6 Catalytic Properties

The coupling of carbon dioxide and epoxides catalyzed by salicylaldiminato-Cu(II) (Scheme 2) was investigated under different reaction conditions. The results were shown in Fig. 4 and Table 4. The yields of cyclic carbonates with respect to the corresponding epoxides were determined by comparing the ratio of product to substrate in the ^1H NMR spectrum of an aliquot of the reaction mixture. It can be seen that the $[\text{Cu}_3(\text{L}_2)_4\text{Cl}_2 \cdot \text{CuCl}_2$ has a better catalytic activity than from the other Cu(II) complexes for the formation of cyclic organic carbonates from carbon dioxide (Fig. 4). Selectively very high conversion (TON = 30,335) was obtained while using this catalyst ($[\text{Cu}_3(\text{L}_2)_4\text{Cl}_2 \cdot \text{CuCl}_2$) and epichlorohydrine as the substrate. The results shown that the multinuclear Cu(II) salicylaldiminato complexes $[\text{Cu}_3(\text{L}_2)_4\text{Cl}_2 \cdot \text{CuCl}_2$ and $[\text{Cu}_3(\text{L}_3)_4\text{Cl}_2 \cdot \text{CuCl}_2$ are more efficient than the other $[\text{Cu}(\text{L}_1)_2]$ metal complex which differs from the containing the allyl substituent instead of pyridine ring. Additional solvent such as dichloromethane are found to be useless for catalytic runs (compare Table 4, entry 5 and 6) [41].

The catalyst $[\text{Cu}_3(\text{L}_2)_4\text{Cl}_2 \cdot \text{CuCl}_2$ shows low activity without additives of DMAP that can enhance the Lewis acidity of Cu metal centre. To ascertain the activity of DMAP alone in this reaction under the given conditions the catalytic blank-run without Cu(II) catalyst was done and found to be 5% conversion (Table 4, entry 1). According to this result it can be understood metal catalyst must be used with a Lewis base such as DMAP. A comparative study with DMAP and NEt_3 was investigated. DMAP is more active base with 47% yield (Table 4, entry 7), the yield is

Fig. 4 The comparison of metal catalysts for the formation of 1,2-epoxy butane to corresponding cyclic carbonate at the same catalytic conditions; reaction conditions: Cu(II) complexes (1.125×10^{-5} mol), 1,2-epoxy butane (4.5×10^{-2} mol), DMAP (9×10^{-5} mol), CO_2 (1.6 Mpa), 100°C , 2 h

**Table 4**

Entries	Epoxide	Time (hour)	Temp. $^\circ\text{C}$	Solvent	Yield (%) ^a	Selectivity (%)	TON ^b
1.	PO	2	100	—	5.0 ^c	95	50
2.	PO	1	80	—	7.3 ^d	96	7
3.	EC	2	100	—	98.3	98	3932
4.	EC	6	100	—	90.7	98	30,335 [*]
5.	EB	2	100	CH_2Cl_2	60.0	98	2400
6.	EB	2	100	—	76.3	96	3052
7.	PO	2	100	—	46.9	99	1876
8.	PO	4	100	—	53.0	99	2120
9.	PO	6	100	—	64.7	98	2588
10.	PO	10	100	—	87.0	98	3480
11.	PO	12	100	—	88.6	97	3544
12.	PO	2	100	—	34 ^e	94	340
13.	SO	2	100	—	83.0	92	3320
14.	SO	4	100	—	95.0	89	3800

R Propylene oxide (PO), epichlorohydrine (EC), styrene oxide (SO) and 1,2-epoxy butane (EB)

* 2.99×10^{-5} mol $[\text{Cu}_3(\text{L}_2)_4]\text{Cl}_2 \cdot \text{CuCl}_2$ was used as the catalyst; 100 mmol (7.8 mL) epichlorohydrin was used as the substrate; 5.98×10^{-5} mol DMAP was used as the base

^a Yield of epoxides to corresponding cyclic carbonates was determined by comparing the ratio of product to substrate in the ^1H NMR spectrum of an aliquot of the reaction mixture

^b Moles of cyclic carbonate produced per mole of catalyst

^c Blank run, without any Cu(II) complex as catalyst

^d Et_3N was used as base

^e $\text{CuCl}_2 \cdot \text{H}_2\text{O}$ (4.5×10^{-5} mol) was used as the catalyst

decreased to 7% yield (Table 4, entry 2) when NEt_3 was replaced as base while using the PO as the substrate.

Meanwhile the electron-withdrawing groups at the 2-position of the epoxide activated the substrate, while electron-donating substituents deactivate the epoxide (Table 4). The epoxides (1,2-epoxybutane, propylene oxide, styrene oxide, epichlorohydrin) were tested as

substrates and epichlorohydrin was found to be the most reactive epoxide, while propylene epoxide exhibited the lowest activity of the epoxides surveyed in accordance with previous study [21]. The active catalyst contains trimetallic species of the copper in it. In order to see the effect of $[\text{CuCl}_2]$ on the activation of CO_2 , the blank run was performed (Table 4, entry 12). As can be seen from the table

only 34% cyclic carbonate yield was obtained. This result shows that the independent $\text{CuCl}_2 \cdot \text{H}_2\text{O}$ salt is not effective alone. The whole complex $[\text{Cu}_3(\text{L}_2)_4]\text{Cl}_2 \cdot \text{CuCl}_2$ showed activity. The influence of time on the yield of propylene carbonate (PC) was investigated at CO_2 pressures of 1.6 MPa. The yield increased with increasing the catalytic reaction time (Table 4).

Although the metal centres are different (copper and ruthenium), the reaction mechanism we envisioned the occurrence of a similar pathway to the one proposed previously [42], i.e. activation of the epoxide by a Lewis acid and attacks of Lewis base (DMAP) to the sterically less hindered carbon atom to open the epoxide ring. The generated oxy anion species then reacts with CO_2 to give the cyclic carbonate.

4 Conclusion

New salicylaldimine ligands (L_1H , L_2H and L_3H) with their mono or multinuclear Cu(II) complexes were synthesized. Besides the classical methods such as FT-IR, UV-Vis, $^1\text{H-NMR}$, elemental analysis, and X-ray structural determination in addition to magnetic susceptibility techniques for structural characterization. The synthesized steric hindered salen type complexes tested as catalysts for the formation of cyclic carbonates from CO_2 and liquid epoxides. The results showed that the multinuclear Cu(II) salicylaldiminato complexes $[\text{Cu}_3(\text{L}_2)_4]\text{Cl}_2 \cdot \text{CuCl}_2$ and $[\text{Cu}_3(\text{L}_3)_4]\text{Cl}_2 \cdot \text{CuCl}_2$ are more efficient than the other $[\text{Cu}(\text{L}_1)_2]$ metal complex which differs from the containing the ally substituent instead of pyridine ring. Very high conversion (TON = 30,335) was obtained while using this catalyst ($[\text{Cu}_3(\text{L}_2)_4]\text{Cl}_2 \cdot \text{CuCl}_2$) and epichlorohydrine as the substrate.

5 Supplementary Material

CCDC 759981 contains the supplementary crystallographic data for this paper. These data can be obtained free of charge from The Cambridge Crystallographic Data Centre via www.ccdc.cam.ac.uk/data_request/cif.

Acknowledgments The authors wish to acknowledge the Faculty of Arts and Sciences, Ondokuz Mayıs University, Turkey, for the use of the Stoe IPDS-II diffractometer (purchased from Grant No. F279 of the University Research Fund).

References

- Kember MR, White AJP, Williams CK (2009) Inorg Chem 48:9535
- Coates GW, Moore DR (2004) Angew Chem Int Ed 43:6618
- Darensbourg DJ, Ulusoy M, Karonnirun O, Poland RR, Reibenspies JH, Çetinkaya B (2009) Macromolecules 42:6992
- Gibson DH (1996) Chem Rev 96:2063
- Miao CX, Wang JQ, Wu Y, Du Y, He LN (2008) ChemSusChem 1:236
- Kendall JL, Canelas DA, Young JL, DeSimone JM (1999) Chem Rev 99:54
- Darensbourg DJ, Holtcamp MW (1996) Coord Chem Rev 153:155
- Inoue S (1976) Chemtech 6:588
- Beckman EJ (1999) Science 283:946
- Lu XB, Shi L, Wang Y, Zhang R, Zhang YJ, Peng XJ, Zhang ZC, Li B (2006) J Am Chem Soc 128:1664
- Jung JH, Ree M, Chang T (1999) J Polym Sci Part A Polym Chem 37:3329
- Aida T, Ishikawa M, Inoue S (1986) Macromolecules 19:8
- Shaikh AAG, Sivaram S (1996) Chem Rev 96:951
- Sakakura T, Kohno K (2009) Chem Commun 11:1312
- Mette M, Mikkel J, Frederik CK (2010) Energy Environ Sci 3:43
- Xiaoding X, Moulijn JA (1996) Energy Fuels 10:05
- Zeherhoven R, Eloneva S, Teir S (2006) Catal Today 115:73
- Pachero MA, Marshall CL (1997) Energy Fuels 11:2
- Kanmani Raja K, Eswaramoorthy D, Kutti Ranib S, Rajeshc J, Jorapur Y, Thambidurai S, Athappanc PR, Rajagopala G (2009) J Mol Catal A Chem 303:52
- Choi JC, Kohno K, Ohshima Y, Yasuda H, Sakakura T (2008) Cataly Commun 9(7):1630
- Miller JA, Gross BA, Zhuravel MA, Jin W, Nguyen ST (2005) Angew Chem Int Ed 44:3885
- Kilic A, Ulusoy M, Durgun M, Tasci Z, Yilmaz I, Cetinkaya B (2010) Appl Organometal Chem 24:446
- Earnshaw A (1968) Introduction to magnetochemistry. Academic Press, London, p 4
- Sheldrick GM (1997) SHELXS-97—a program for automatic solution of crystal structures. University of Gottingen, Germany
- Farrugia LJ (1998) WINGX—a windows program for crystal structure analysis. University of Glasgow, Glasgow
- Farrugia LJ (1997) J Appl Crystallogr 30:565
- Spek AL (2005) PLATON—a multipurpose crystallographic tool. Utrecht University, Utrecht,
- Kilic A, Tas E, Deveci B, Yilmaz I (2007) Polyhedron 26:4009
- Tas E, Kilic A, Durgun M, Yilmaz I, Ozdemir I, Gurbuz N (2009) J Organomet Chem 694:446
- Ulusoy M, Sahin O, Buyukgungor O, Cetinkaya B (2008) J Organomet Chem 693:1895
- Kılınçarslan R, Karabıyık H, Ulusoy M, Aygün M, Çetinkaya B, Büyükgüngör O (2006) J Coord Chem 59:1649
- Kilic A, Tas E, Gumgum B, Yilmaz I (2007) Heteroatom Chem 18:657
- Li Y, Yang ZY (2009) Inorg Chim Acta 13:4823
- Shit S, Chakraborty J, Samanta B, Slawin AMZ, Gramlich V, Mitra S (2009) Struct Chem 20:633
- Sacconi L, Ciampolini M, Maffio F, Cavasino FP (1962) J Am Chem Soc 84:3246
- Carlin RL (1965) Trans Met Chem. Marcel Dekker, New York, vol 1
- Tas E, Ulusoy M, Guler M, Yilmaz I (2004) Trans Met Chem 29:180
- Pui A, Mahy JP (2007) Polyhedron 26:3143
- Ilhan S, Temel H, Kilic A (2008) J Coord Chem 61(2):277
- Bernstein J, Davis RE, Shimon L, Chang NL (1995) Angew Chem Int Ed Engl 34:1555
- Ulusoy M, Cetinkaya E, Cetinkaya B (2009) Appl Organometal Chem 23:68
- Bu Z, Qin G, Cao S (2007) J Mol Cat A 277:35